



A mathematical theory of semantic development in deep neural networks

Andrew M. Saxe^{a,1}, James L. McClelland^b, and Surya Ganguli^{c,d}

^aDepartment of Experimental Psychology, University of Oxford, Oxford OX2 6GG, United Kingdom; ^bDepartment of Psychology, Stanford University, Stanford, CA 94305; ^cDepartment of Applied Physics, Stanford University, Stanford, CA 94305; and ^dGoogle Brain, Google, Mountain View, CA 94043

Edited by Terrence J. Sejnowski, Salk Institute for Biological Studies, La Jolla, CA, and approved April 9, 2019 (received for review December 6, 2018)

An extensive body of empirical research has revealed remarkable regularities in the acquisition, organization, deployment, and neural representation of human semantic knowledge, thereby raising a fundamental conceptual question: What are the theoretical principles governing the ability of neural networks to acquire, organize, and deploy abstract knowledge by integrating across many individual experiences? We address this question by mathematically analyzing the nonlinear dynamics of learning in deep linear networks. We find exact solutions to this learning dynamics that yield a conceptual explanation for the prevalence of many disparate phenomena in semantic cognition, including the hierarchical differentiation of concepts through rapid developmental transitions, the ubiquity of semantic illusions between such transitions, the emergence of item typicality and category coherence as factors controlling the speed of semantic processing, changing patterns of inductive projection over development, and the conservation of semantic similarity in neural representations across species. Thus, surprisingly, our simple neural model qualitatively recapitulates many diverse regularities underlying semantic development, while providing analytic insight into how the statistical structure of an environment can interact with nonlinear deep-learning dynamics to give rise to these regularities.

semantic cognition | deep learning | neural networks | generative models

Human cognition relies on a rich reservoir of semantic knowledge, enabling us to organize and reason about our complex sensory world (1–4). This semantic knowledge allows us to answer basic questions from memory (e.g., “Do birds have feathers?”) and relies fundamentally on neural mechanisms that can organize individual items, or entities (e.g., *canary* or *robin*), into higher-order conceptual categories (e.g., *birds*) that include items with similar features, or properties. This knowledge of individual entities and their conceptual groupings into categories or other ontologies is not present in infancy, but develops during childhood (1, 5), and in adults, it powerfully guides inductive generalizations.

The acquisition, organization, deployment, and neural representation of semantic knowledge has been intensively studied, yielding many well-documented empirical phenomena. For example, during acquisition, broader categorical distinctions are generally learned before finer-grained distinctions (1, 5), and periods of relative stasis can be followed by abrupt conceptual reorganization (6, 7). Intriguingly, during these periods of developmental stasis, children can believe illusory, incorrect facts about the world (2).

Also, many psychophysical studies of performance in semantic tasks have revealed empirical regularities governing the organization of semantic knowledge. In particular, category membership is a graded quantity, with some items being more or less typical members of a category (e.g., a sparrow is a more typical bird than a penguin). Item typicality is reproducible across individuals (8, 9) and correlates with performance on a diversity of semantic tasks (10–14). Moreover, certain categories themselves are thought to be highly coherent (e.g., the set of things that are *dogs*), in contrast to less coherent categories (e.g., the set of things that are *blue*). More coherent categories play a privileged role in the organization of our semantic knowledge; coherent categories are the ones that are most easily learned and represented (8, 15, 16). Also, the organization of semantic knowledge power-

fully guides its deployment in novel situations, where one must make inductive generalizations about novel items and properties (2, 3). Indeed, studies of children reveal that their inductive generalizations systematically change over development, often becoming more specific with age (2, 3, 17–19).

Finally, recent neuroscientific studies have probed the organization of semantic knowledge in the brain. The method of representational similarity analysis (20, 21) revealed that the similarity structure of cortical activity patterns often reflects the semantic similarity structure of stimuli (22, 23). And, strikingly, such neural similarity structure is preserved across humans and monkeys (24, 25).

This wealth of empirical phenomena raises a fundamental conceptual question about how neural circuits, upon experiencing many individual encounters with specific items, can, over developmental time scales, extract abstract semantic knowledge consisting of useful categories that can then guide our ability to reason about the world and inductively generalize. While several theories have been advanced to explain semantic development, there is currently no analytic, mathematical theory of neural circuits that can account for the diverse phenomena described above. Interesting nonneural accounts for the discovery of abstract semantic structure include the conceptual “theory-theory” (2, 17, 18) and computational Bayesian (26) approaches. However, neither currently proposes a neural implementation that can infer abstract concepts from a stream of examples. Also, they hold that specific domain theories or a set of candidate structural forms must be available a priori for learning to occur. In contrast, much prior work has shown, through simulations, that neural networks can gradually extract semantic

Significance

Over the course of development, humans learn myriad facts about items in the world, and naturally group these items into useful categories and structures. This semantic knowledge is essential for diverse behaviors and inferences in adulthood. How is this richly structured semantic knowledge acquired, organized, deployed, and represented by neuronal networks in the brain? We address this question by studying how the nonlinear learning dynamics of deep linear networks acquires information about complex environmental structures. Our results show that this deep learning dynamics can self-organize emergent hidden representations in a manner that recapitulates many empirical phenomena in human semantic development. Such deep networks thus provide a mathematically tractable window into the development of internal neural representations through experience.

Author contributions: A.M.S., J.L.M., and S.G. designed research; A.M.S. and S.G. performed research; and A.M.S., J.L.M., and S.G. wrote the paper.

The authors declare no conflict of interest.

This article is a PNAS Direct Submission.

Published under the PNAS license.

¹To whom correspondence should be addressed. Email: andrew.saxe@psy.ox.ac.uk.

This article contains supporting information online at www.pnas.org/lookup/suppl/doi:10.1073/pnas.1802261116/-DCSupplemental.

Published online May 17, 2019.

structure by incrementally adjusting synaptic weights via error-corrective learning (4, 27–32). However, the theoretical principles governing how even simple artificial neural networks extract semantic knowledge from their ongoing stream of experience, embed this knowledge in their synaptic weights, and use these weights to perform inductive generalization, remain obscure.

In this work, our goal is to fill this gap by using a simple class of neural networks—namely, deep linear networks. Surprisingly, this model class can learn a wide range of distinct types of structure without requiring either initial domain theories or a prior set of candidate structural forms, and accounts for a diversity of phenomena involving semantic cognition described above. Indeed, we build upon a considerable neural network literature (27–32) addressing such phenomena through simulations of more complex nonlinear networks. We build particularly on the integrative, simulation-based treatment of semantic cognition in ref. 4, often using the same modeling strategy in a simpler linear setting, to obtain similar results but with additional analytical insight. In contrast to prior work, whether conceptual, Bayesian, or connectionist, our simple model permits exact analytical solutions describing the entire developmental trajectory of knowledge acquisition and organization and its subsequent impact on the deployment and neural representation of semantic structure. In the following, we describe semantic knowledge acquisition, organization, deployment, and neural representation in sequence, and we summarize our main findings in *Discussion*.

A Deep Linear Neural Network Model

Here, we consider a framework for analyzing how neural networks extract semantic knowledge by integrating across many individual experiences of items and their properties, across developmental time. In each experience, given an item as input, the network is trained to produce its associated properties or features as output. Consider, for example, the network's interaction with the semantic domain of living things, schematized in Fig. 1*A*. If the network encounters an item, such as a *canary*, perceptual neural circuits produce an activity vector $\mathbf{x} \in \mathbb{R}^{N_1}$ that identifies this item and serves as input to the semantic system. Simultaneously, the network observes some of the item's properties—for example, that a canary *can fly*. Neural circuits produce an activity feature vector $\mathbf{y} \in \mathbb{R}^{N_3}$ of that item's properties which serves as the desired output of the semantic network. Over time, the network experiences many such episodes with different items and their properties. The total collected experience furnished by the environment to the semantic system is thus a set of P examples $\{\mathbf{x}^i, \mathbf{y}^i\}$, $i = 1, \dots, P$, where the input vector \mathbf{x}^i identifies item i , and the output vector \mathbf{y}^i is a set of features to be associated with this item.

The network's task is to predict an item's properties \mathbf{y} from its perceptual representation \mathbf{x} . These predictions are generated by propagating activity through a three-layer linear neural network (Fig. 1*B*). The input activity pattern \mathbf{x} in the first layer propagates through a synaptic weight matrix \mathbf{W}^1 of size $N_2 \times N_1$, to

create an activity pattern $\mathbf{h} = \mathbf{W}^1 \mathbf{x}$ in the second layer of N_2 neurons. We call this layer the “hidden” layer because it corresponds neither to input nor output. The hidden-layer activity then propagates to the third layer through a second synaptic weight matrix \mathbf{W}^2 of size $N_3 \times N_2$, producing an activity vector $\hat{\mathbf{y}} = \mathbf{W}^2 \mathbf{h}$ which constitutes the output prediction of the network. The composite function from input to output is thus simply $\hat{\mathbf{y}} = \mathbf{W}^2 \mathbf{W}^1 \mathbf{x}$. For each input \mathbf{x} , the network compares its predicted output $\hat{\mathbf{y}}$ to the observed features \mathbf{y} , and it adjusts its weights so as to reduce the discrepancy between \mathbf{y} and $\hat{\mathbf{y}}$.

To study the impact of depth, we will contrast the learning dynamics of this deep linear network to that of a shallow network that has just a single weight matrix, \mathbf{W}^s of size $N_3 \times N_1$ linking input activities directly to the network's predictions $\hat{\mathbf{y}} = \mathbf{W}^s \mathbf{x}$. It may seem that there is no utility in considering deep linear networks, since the composition of linear functions remains linear. Indeed, the appeal of deep networks is thought to lie in the increasingly expressive functions they can represent by successively cascading many layers of nonlinear elements (33). In contrast, deep linear networks gain no expressive power from depth; a shallow network can compute any function that the deep network can, by simply taking $\mathbf{W}^s = \mathbf{W}^2 \mathbf{W}^1$. However, as we see below, the learning dynamics of the deep network is highly nonlinear, while the learning dynamics of the shallow network remains linear. Strikingly, many complex, nonlinear features of learning appear even in deep linear networks and do not require neuronal nonlinearities.

To illustrate the power of deep linear networks to capture learning dynamics, even in nonlinear networks, we compare the two learning dynamics in Fig. 2. Fig. 2*A* shows a low-dimensional visualization of the simulated learning dynamics of a multilayered nonlinear neural network trained to predict the properties of a set of items in a semantic domain of animals and plants (for details of the neural architecture and training data see ref. 4). The nonlinear network exhibits a striking, hierarchical, progressive differentiation of structure in its internal hidden representations, in which animals vs. plants are first distinguished, then birds vs. fish and trees vs. flowers, and, finally, individual items. This remarkable phenomenon raises important questions about the theoretical principles governing the hierarchical differentiation of structure in neural networks: How and why do the network's dynamics and the statistical structure of the input conspire to generate this phenomenon? In Fig. 2*B*, we mathematically derive this phenomenon by finding analytic solutions to the nonlinear dynamics of learning in a deep linear network, when that network is exposed to a hierarchically structured semantic domain, thereby shedding theoretical insight onto the origins of hierarchical differentiation in a deep network. We present the derivation below, but for now, we note that the resemblance in Fig. 2 suggests that deep linear networks can form an excellent, analytically tractable model for shedding conceptual insight into the learning dynamics, if not the expressive power, of their nonlinear counterparts.

Acquiring Knowledge

We now outline the derivation that leads to Fig. 2*B*. The incremental error-corrective process described above can be formalized as online stochastic gradient descent; each time an example i is presented, the weights \mathbf{W}^2 and \mathbf{W}^1 receive a small adjustment in the direction that most rapidly decreases the squared error $\|\mathbf{y}^i - \hat{\mathbf{y}}^i\|^2$, yielding the standard back propagation learning rule

$$\Delta \mathbf{W}^1 = \lambda \mathbf{W}^{2T} (\mathbf{y}^i - \hat{\mathbf{y}}^i) \mathbf{x}^{iT}, \quad \Delta \mathbf{W}^2 = \lambda (\mathbf{y}^i - \hat{\mathbf{y}}^i) \mathbf{h}^{iT}, \quad [1]$$

where λ is the learning rate. This incremental update depends only on experience with a single item, leaving open the fundamental question of how and when the accumulation of such incremental updates can extract over developmental time abstract structures, like hierarchical taxonomies, that are emergent properties of the entire domain of items and their features.

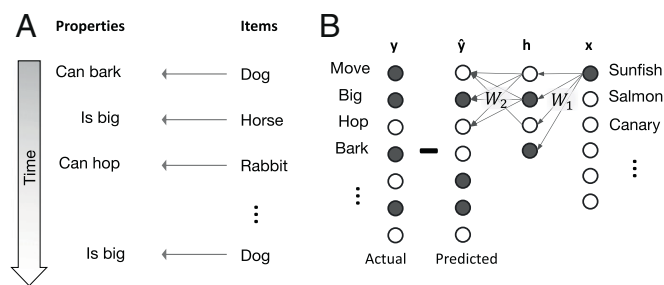


Fig. 1. (A) During development, the network experiences sequential episodes with items and their properties. (B) After each episode, the network adjusts its synaptic weights to reduce the discrepancy between actual observed properties \mathbf{y} and predicted properties $\hat{\mathbf{y}}$.

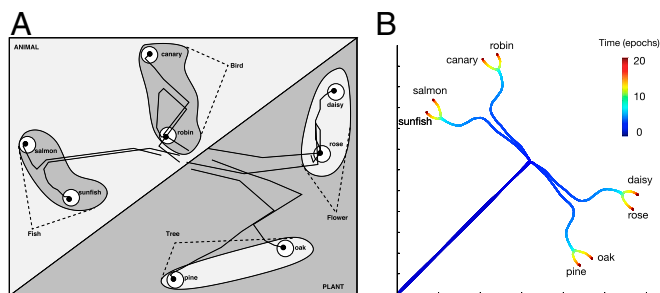


Fig. 2. (A) A two-dimensional multidimensional scaling (MDS) visualization of the temporal evolution of internal representations, across developmental time, of a deep nonlinear neural network studied in ref. 4. Reprinted with permission from ref. 4. (B) An MDS visualization of analytically derived learning trajectories of the internal representations of a deep linear network exposed to a hierarchically structured domain.

We show that the extraction of such abstract domain structure is possible, provided learning is gradual, with a small learning rate λ . In this regime, many examples are seen before the weights appreciably change, so learning is driven by the statistical structure of the domain. We imagine training is divided into a sequence of learning epochs. In each epoch, the above rule is followed for all P examples in random order. Then, averaging [1] over all P examples and taking a continuous time limit gives the mean change in weights per learning epoch,

$$\tau \frac{d}{dt} \mathbf{W}^1 = \mathbf{W}^{2T} (\Sigma^{yx} - \mathbf{W}^2 \mathbf{W}^1 \Sigma^x), \quad [2]$$

$$\tau \frac{d}{dt} \mathbf{W}^2 = (\Sigma^{yx} - \mathbf{W}^2 \mathbf{W}^1 \Sigma^x) \mathbf{W}^1 T, \quad [3]$$

where $\Sigma^x \equiv E[\mathbf{x}\mathbf{x}^T]$ is an $N_1 \times N_1$ input correlation matrix, $\Sigma^{yx} \equiv E[\mathbf{y}\mathbf{x}^T]$ is an $N_3 \times N_1$ input–output correlation matrix, and $\tau \equiv \frac{1}{P\lambda}$ (see *SI Appendix*). Here, t measures time in units of learning epochs. These equations reveal that learning dynamics, even in our simple linear network, can be highly complex: The second-order statistics of inputs and outputs drives synaptic weight changes through coupled nonlinear differential equations with up to cubic interactions in the weights.

Explicit Solutions from Tabula Rasa. These nonlinear dynamics are difficult to solve for arbitrary initial conditions. However, we are interested in a particular limit: learning from a state of essentially no knowledge, which we model as small random synaptic weights. To further ease the analysis, we shall assume that the influence of perceptual correlations is minimal ($\Sigma^x \approx \mathbf{I}$). Our goal, then, is to understand the dynamics of learning in [2] and [3] as a function of the input–output correlation matrix Σ^{yx} . The learning dynamics is tied to terms in the singular value decomposition (SVD) of Σ^{yx} (Fig. 3A),

$$\Sigma^{yx} = \mathbf{U}\mathbf{S}\mathbf{V}^T = \sum_{\alpha=1}^{\min(N_1, N_3)} s_{\alpha} \mathbf{u}^{\alpha} \mathbf{v}^{\alpha T}, \quad [4]$$

which decomposes any matrix into the product of three matrices. Each of these matrices has a distinct semantic interpretation.

For example, the α 'th column \mathbf{v}^{α} of the $N_1 \times N_1$ orthogonal matrix \mathbf{V} can be thought of as an object-analyzer vector; it determines the position of item i along an important semantic dimension α in the training set through the component v_i^{α} . To illustrate this interpretation concretely, we consider a simple example dataset with four items (*canary*, *salmon*, *oak*, and *rose*) and five properties (Fig. 3). The two animals share the property *can move*, while the two plants do not. Also, each item has a unique property: *can fly*, *can swim*, *has bark*, and *has petals*. For this dataset, while the first row of \mathbf{V}^T is a uniform mode, the second row, or the second object-analyzer vector \mathbf{v}^2 , determines where items sit on an *animal–plant* dimension and hence

has positive values for the *canary* and *salmon* and negative values for the plants. The other dimensions identified by the SVD are a *bird–fish* dimension and a *flower–tree* dimension.

The corresponding α 'th column \mathbf{u}^{α} of the $N_3 \times N_3$ orthogonal matrix \mathbf{U} can be thought of as a feature-synthesizer vector for semantic distinction α . Its components u_m^{α} indicate the extent to which feature m is present or absent in distinction α . Hence, the feature synthesizer \mathbf{u}^2 associated with the *animal–plant* semantic dimension has positive values for *move* and negative values for *roots*, as animals typically can move and do not have roots, while plants behave oppositely. Finally, the $N_3 \times N_1$ singular value matrix \mathbf{S} has nonzero elements $s_{\alpha}, \alpha = 1, \dots, N_1$ only on the diagonal, ordered so that $s_1 \geq s_2 \geq \dots \geq s_{N_1}$. s_{α} captures the overall strength of the α 'th dimension. The large singular value for the *animal–plant* dimension reflects the fact that this one dimension explains more of the training set than the finer-scale dimensions *bird–fish* and *flower–tree*.

Given the SVD of the training set's input–output correlation matrix in [4], we can now explicitly describe the network's learning dynamics. The network's overall input–output map at time t is a time-dependent version of this SVD (Fig. 3B); it shares the object-analyzer and feature-synthesizer matrices of the SVD of Σ^{yx} , but replaces the singular value matrix \mathbf{S} with an effective singular value matrix $\mathbf{A}(t)$,

$$\mathbf{W}^2(t)\mathbf{W}^1(t) = \mathbf{U}\mathbf{A}(t)\mathbf{V}^T = \sum_{\alpha=1}^{N_2} a_{\alpha}(t) \mathbf{u}^{\alpha} \mathbf{v}^{\alpha T}, \quad [5]$$

where the trajectory of each effective singular value $a_{\alpha}(t)$ obeys

$$a_{\alpha}(t) = \frac{s_{\alpha} e^{2s_{\alpha} t / \tau}}{e^{2s_{\alpha} t / \tau} - 1 + s_{\alpha} / a_{\alpha}^0}. \quad [6]$$

Eq. 6 describes a sigmoidal trajectory that begins at some initial value a_{α}^0 at time $t=0$ and rises to s_{α} as $t \rightarrow \infty$, as plotted

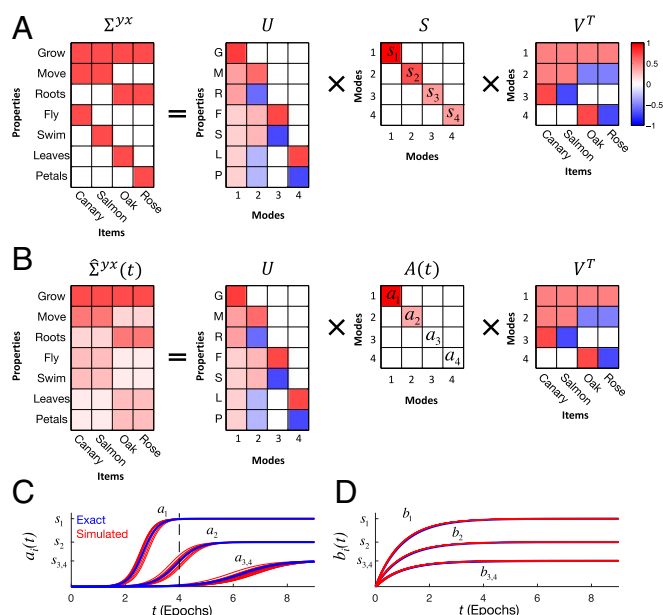


Fig. 3. (A) SVD of input–output correlations. Associations between items and their properties are decomposed into modes. Each mode links a set of properties (a column of \mathbf{U}) with a set of items (a row of \mathbf{V}^T). The strength of the mode is encoded by the singular value (diagonal element of \mathbf{S}). (B) Network input–output map, analyzed via the SVD. The effective singular values (diagonal elements of $\mathbf{A}(t)$) evolve over time during learning. (C) Trajectories of the deep network's effective singular values $a_i(t)$. The black dashed line marks the point in time depicted in B. (D) Time-varying trajectories of a shallow network's effective singular values $b_i(t)$.

in Fig. 3C. This solution is applicable when the network begins from an undifferentiated state with little initial knowledge corresponding to small random initial weights (see *SI Appendix*), and it provides an accurate description of the learning dynamics in this regime, as confirmed by simulation in Fig. 3C. The dynamics in Eq. 6 for one hidden layer can be generalized to multiple hidden layers (*SI Appendix*). Moreover, while we have focused on the case of no perceptual correlations, in *SI Appendix*, we examine a special case of how perceptual correlations and semantic task structure interact to determine learning speed. We find that perceptual correlations can either speed up or slow down learning, depending on whether they are aligned or misaligned with the input dimensions governing task-relevant semantic distinctions.

This solution also gives insight into how the internal representations in the hidden layer of the deep network evolve. An exact solution for \mathbf{W}^2 and \mathbf{W}^1 is given by

$$\mathbf{W}^1(t) = \mathbf{Q}\sqrt{\mathbf{A}(t)}\mathbf{V}^T, \quad \mathbf{W}^2(t) = \mathbf{U}\sqrt{\mathbf{A}(t)}\mathbf{Q}^{-1}, \quad [7]$$

where \mathbf{Q} is an arbitrary $N_2 \times N_2$ invertible matrix (*SI Appendix*). If initial weights are small, then the matrix \mathbf{Q} will be close to orthogonal, i.e., $\mathbf{Q} \approx \mathbf{R}$, where $\mathbf{R}^T \mathbf{R} = \mathbf{I}$. Thus, the internal representations are specified up to an arbitrary rotation \mathbf{R} . Factoring out the rotation, the hidden representation of item i is

$$h_i^\alpha(t) = \sqrt{a^\alpha(t)} \mathbf{v}_i^\alpha. \quad [8]$$

Thus, internal representations develop by projecting inputs onto more and more input-output modes as they are learned.

The shallow network has an analogous solution, $\mathbf{W}^s(t) = \sum_{\alpha=1}^{\min(N_1, N_3)} b_\alpha(t) \mathbf{u}^\alpha \mathbf{v}^{\alpha T}$, but each singular value obeys

$$b_\alpha(t) = s_\alpha \left(1 - e^{-t/\tau}\right) + b_\alpha^0 e^{-t/\tau}. \quad [9]$$

In contrast to the deep network's sigmoidal trajectory, Eq. 9 describes a simple exponential approach to s_α , as plotted in Fig. 3D. Hence, depth fundamentally changes the learning dynamics, yielding several important consequences below.

Rapid Stage-Like Transitions Due to Depth. We first compare the time course of learning in deep vs. shallow networks as revealed in Eqs. 6 and 9. For the deep network, beginning from a small initial condition $a_\alpha^0 = \epsilon$, each mode's effective singular value $a_\alpha(t)$ rises to within ϵ of its final value s_α in time

$$t(s_\alpha, \epsilon) = \frac{\tau}{s_\alpha} \ln \frac{s_\alpha}{\epsilon}, \quad [10]$$

in the limit $\epsilon \rightarrow 0$ (*SI Appendix*). This is $O(1/s_\alpha)$ up to a logarithmic factor. Hence, modes with stronger explanatory power, as quantified by the singular value, are learned more quickly. Moreover, when starting from small initial weights, the sigmoidal transition from no knowledge of the mode to perfect knowledge can be arbitrarily sharp. Indeed, the ratio of time spent in the sigmoidal transition regime to time spent before making the transition can go to zero as the initial weights go to zero (*SI Appendix*). Thus, rapid stage-like transitions in learning can be prevalent, even in deep linear networks.

By contrast, the shallow-network learning timescale is

$$t(s_\alpha, \epsilon) = \tau \ln \frac{s_\alpha}{\epsilon}, \quad [11]$$

which is $O(1)$ up to a logarithmic factor. Here, the timescale of learning a mode depends only weakly on its associated singular value. Essentially all modes are learned simultaneously, with an exponential rather than sigmoidal learning curve.

Progressive Differentiation of Hierarchical Structure. We are now almost ready to explain how we analytically derive the result in

Fig. 2B. The only remaining ingredient is a mathematical description of the training data. Indeed, the numerical results in Fig. 2A arise from a toy training set, making it difficult to understand how structure in data drives learning. Here, we introduce a probabilistic generative model to reveal general principles of how statistical structure impacts learning. We begin with hierarchical structure, but subsequently show how diverse structures come to be learned by the network (compare Fig. 9).

We use a generative model corresponding to a branching diffusion process that mimics evolutionary dynamics to create an explicitly hierarchical dataset (*SI Appendix*). In the model, each feature diffuses down an evolutionary tree (Fig. 4A), with a small probability of mutating along each branch. The items lie at the leaves of the tree, and the generative process creates a hierarchical similarity matrix between items such that items with a more recent common ancestor on the tree are more similar to each other (Fig. 4B). We analytically compute the SVD of this dataset, and find that the object-analyzer vectors, which can be viewed as functions on the leaves of the tree in Fig. 4C, respect the hierarchical branches of the tree, with the larger singular values corresponding to broader distinctions. In Fig. 4A, we artificially label the leaves and branches of the evolutionary tree with organisms and categories that might reflect a natural realization of this evolutionary process.

Now, inserting the singular values in Fig. 4D (and *SI Appendix*) into the deep-learning dynamics in Eq. 6 to obtain the time-dependent singular values $a^\alpha(t)$, and then inserting these along with the object analyzers vectors \mathbf{v}^α in Fig. 4C into Eq. 8, we obtain a complete analytic derivation of the development of internal representations in the deep network. An MDS visualization of these evolving hidden representations then yields Fig. 2B, which qualitatively recapitulates the much more complex network and dataset that leads to Fig. 2A. In essence, this analysis completes a mathematical proof that the striking progressive differentiation of hierarchical structure observed in Fig. 2 is an inevitable consequence of deep-learning dynamics, even in linear networks, when exposed to hierarchically structured data. The essential intuition is that dimensions of feature variation across items corresponding to broader hierarchical distinctions have stronger statistical structure, as quantified by the singular values of the training data, and hence are learned faster, leading to waves of differentiation in a deep but not shallow network. This pattern of hierarchical differentiation has long been argued to apply to the conceptual development of infants and children (1, 5–7).

Illusory Correlations. Another intriguing aspect of semantic development is that children sometimes attest to false beliefs [e.g., worms have bones (2)] they could not have learned through experience. These errors challenge simple associationist accounts of semantic development that predict a steady, monotonic accumulation of information about individual properties (2, 16, 17, 34). Yet, the network's knowledge of individual properties exhibits

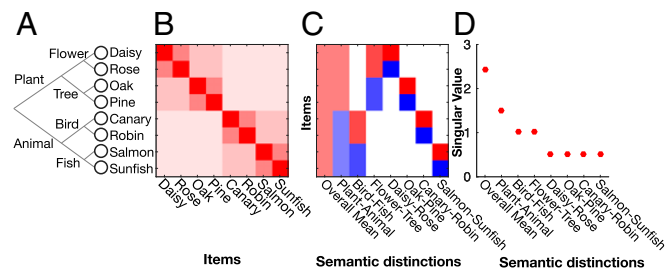


Fig. 4. Hierarchy and the SVD. (A) A domain of eight items with an underlying hierarchical structure. (B) The correlation matrix of the features of the items. (C) SVD of the correlations reveals semantic distinctions that mirror the hierarchical taxonomy. This is a general property of the SVD of hierarchical data. (D) The singular values of each semantic distinction reveal its strength in the dataset and control when it is learned.

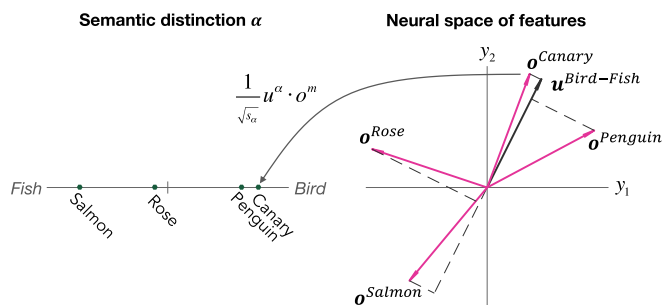


Fig. 6. The geometry of item typicality. For a semantic distinction α (in this case, α is the bird–fish distinction) the object-analyzer vector \mathbf{v}_i^α arranges objects i along an internal neural-representation space, where the most typical birds take the extremal positive coordinates and the most typical fish take the extremal negative coordinates. Objects like a rose, that is neither a bird nor a fish, are located near the origin on this axis. Positions along the neural semantic axis can also be obtained by computing the inner product between the feature vector \mathbf{o}^i for object i and the feature synthesizer \mathbf{u}^α as in [13]. Moreover, \mathbf{u}^α can be thought of as a category prototype for semantic distinction α through [14].

the learned internal representations of the neural network. The typicality of an item with respect to dimension α is the projection of that item's feature vector onto the category prototype in [13]. And the category prototype is an average over all object feature vectors, weighted by their typicality in [14]. Also, in any categorical distinction α , the most typical items i and the most important features m are determined by the extremal values of \mathbf{v}_i^α and \mathbf{u}_m^α . These observations provide a foundation for a more complete future theory of item typicality and category prototypes that can combine information across distinctions at and above a given level.

Category Coherence. The categories we naturally learn are not arbitrary; they are coherent and efficiently represent the structure of the world (8, 15, 16). For example, the set of things that *are red* and *cannot swim* is a well-defined category but, intuitively, is not as coherent as the category of *dogs*; we naturally learn, and even name, the latter category, but not the former. When is a category learned at all, and what determines its coherence? An influential proposal (8, 15) suggested that coherent categories consist of tight clusters of items that share many features and that moreover are highly distinct from other categories with different sets of shared features. Such a definition, as noted in refs. 3, 16, and 17, can be circular: To know which items are category members, one must know which features are important for that category, and, conversely, to know which features are important, one must know which items are members. Thus, a mathematical definition of category coherence that is provably related to the learnability of categories by neural networks has remained elusive. Here, we provide such a definition for a simple model of disjoint categories and demonstrate how neural networks can cut through the Gordian knot of circularity. Our definition and theory are motivated by, and consistent with, prior network simulations exploring notions of category coherence through the coherent covariation of features (4).

Consider, for example, a dataset consisting of N_o objects and N_f features. Now, consider a category consisting of a subset of K_f features that tend to occur with high probability p in a subset of K_o items, whereas a background feature occurs with a lower probability q in a background item when either are not part of the category. For what values of K_f , K_o , p , q , N_f , and N_o can such a category be learned, and how accurately? Fig. 7 A–D illustrates how a neural network can extract three such categories buried in noise. We see in Fig. 7E that the performance of category extraction increases as the number of items K_o and features K_f in the category increases and also as the signal-to-noise ratio, or $\text{SNR} \equiv \frac{(p-q)^2}{q(1-q)}$, increases. Through random matrix theory (SI Appendix), we show that performance depends

on the various parameters *only* through a category coherence variable

$$C = \text{SNR} \frac{K_o K_f}{\sqrt{N_o N_f}}. \quad [15]$$

When the performance curves in Fig. 7E are replotted with category coherence C on the horizontal axis, all of the curves collapse onto a single universal performance curve shown in Fig. 7F. We derive a mathematical expression for this curve in SI Appendix. It displays an interesting threshold behavior: If the coherence $C \leq 1$, the category is not learned at all, and the higher the coherence above this threshold, the better the category is learned.

This threshold is strikingly permissive. For example, at $\text{SNR} = 1$, it occurs at $K_o K_f = \sqrt{N_o N_f}$. Thus, in a large environment of $N_o = 1,000$ objects and $N_f = 1,600$ features, as in Fig. 7A, a small category of 40 objects and 40 features can be easily learned, even by a simple deep linear network. Moreover, this analysis demonstrates how the deep network solves the problem of circularity described above by simultaneously bootstrapping the learning of object analyzers and feature synthesizers in its synaptic weights. Finally, we note that the definition of category coherence in Eq. 15 is qualitatively consistent with previous notions; coherent categories consist of large subsets of items possessing, with high probability, large subsets of features that tend not to cooccur in other categories. However, our quantitative definition has the advantage that it provably governs category-learning performance in a neural network.

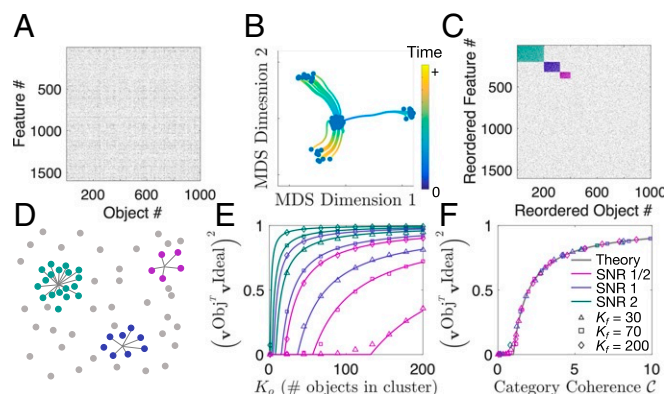


Fig. 7. The discovery of disjoint categories in noise. (A) A dataset of $N_o = 1,000$ items and $N_f = 1,600$ features, with no discernible visible structure. (B) Yet when a deep linear network learns to predict the features of items, an MDS visualization of the evolution of its internal representations reveals three clusters. (C) By computing the SVD of the product of synaptic weights $\mathbf{W}^2 \mathbf{W}^1$, we can extract the network's object analyzers \mathbf{v}^α and feature synthesizers \mathbf{u}^α , finding three with large singular values s_α , for $\alpha = 1, \dots, 3$. Each of these three object analyzers \mathbf{v}^α and feature synthesizers \mathbf{u}^α takes large values on a subset of items and features, respectively, and we can use them to reorder the rows and columns of A to obtain C. This reordering reveals underlying structure in the data corresponding to three disjoint categories, such that if a feature and item belong to a category, the feature is present with a high probability p , whereas if it does not, it appears with a low probability q . (D) Thus, intuitively, the dataset corresponds to three clusters buried in a noise of irrelevant objects and features. (E) Performance in recovering one such category can be measured by computing the correlation coefficients between the object analyzer and feature synthesizer returned by the network to the ideal object analyzer $\mathbf{v}^{\text{ideal}}$ and ideal feature synthesizer $\mathbf{u}^{\text{ideal}}$ that take nonzero values on the items and features, respectively, that are part of the category and are zero on the rest of the items and features. This learning performance, for the object analyzer, is shown for various parameter values. Solid curves are analytically derived from a random matrix analysis (SI Appendix), and data points are obtained from simulations. (F) All performance curves in E collapse onto a single theoretically predicted, universal learning curve, when measured in terms of the category coherence defined in Eq. 15. SNR, signal-to-noise ratio.

Basic Categories. Closely related to category coherence, a variety of studies have revealed a privileged role for basic categories at an intermediate level of specificity (e.g., *bird*), compared with superordinate (e.g., *animal*) or subordinate (e.g., *robin*) levels. At this basic level, people are quicker at learning names (38, 39), prefer to generate names (39), and are quicker to verify the presence of named items in images (11, 39). We note that basic-level advantages typically involve naming tasks done at an older age, and so need not be inconsistent with progressive differentiation of categorical structure from superordinate to subordinate levels as revealed in preverbal cognition (1, 4–7, 40). Moreover, some items are named more frequently than others, and these frequency effects could contribute to a basic-level advantage (4). However, in artificial category-learning experiments with tightly controlled frequencies, basic-level categories are still often learned first (41). What environmental statistics could lead to this effect? While several properties have been proposed (11, 35, 37, 41), a mathematical function of environmental structure that provably confers a basic-level advantage to neural networks has remained elusive.

Here, we provide such a function by generalizing the notion of category coherence \mathcal{C} in the previous section to hierarchically structured categories. Indeed, in any dataset containing strong categorical structure, so that its singular vectors are in one-to-one correspondence with categorical distinctions, we simply propose to define the coherence of a category by the associated singular value. This definition has the advantage of obeying the theorem that more coherent categories are learned faster, through Eq. 6. Moreover, we show in *SI Appendix* that this definition is consistent with that of category coherence \mathcal{C} defined in Eq. 15 for the special case of disjoint categories. However, for hierarchically structured categories, as in Fig. 4, this singular value definition always predicts an advantage for superordinate categories, relative to basic or subordinate. Is there an alternate statistical structure for hierarchical categories that confers high category coherence at lower levels in the hierarchy? We exhibit two such structures in Fig. 8. More generally, in *SI Appendix*, we analytically compute the singular values at each level of the hierarchy in terms of the similarity structure of items. We find that these singular values are a weighted sum of within-cluster similarity minus between-cluster similarity for all levels below, weighted by the fraction of items that are descendants of that level. If at any level, between-cluster similarity is negative, that detracts from the coherence of superordinate categories, contributes strongly to the coherence of categories at that level, and does not contribute to subordinate categories.

Thus, the singular value-based definition of category coherence is qualitatively consistent with prior intuitive notions. For instance, paraphrasing Keil (17), coherent categories are clusters of tight bundles of features separated by relatively empty spaces. Also, consistent with refs. 3, 16, and 17, we note that we cannot judge the coherence of a category without knowing about its relations to all other categories, as singular values are a complex emergent property of the entire environment. But going beyond past intuitive notions, our quantitative definition of category coherence based on singular values enables us to prove that coherent categories are most easily and quickly learned and also provably provide the most accurate and efficient linear representation of the environment, due to the global optimality properties of the SVD (see *SI Appendix* for details).

Capturing Diverse Domain Structures. While we have focused thus far on hierarchical structure, the world may contain many different structure types. Can a wide range of such structures be learned and encoded by neural networks? To study this question, we formalize structure through probabilistic graphical models (PGMs), defined by a graph over items (Fig. 9, top) that can express a variety of structural forms, including clusters, trees, rings, grids, orderings, and hierarchies. Features are assigned to items by independently sampling from the PGM (ref. 26 and *SI Appendix*), such that nearby items in the graph are more likely

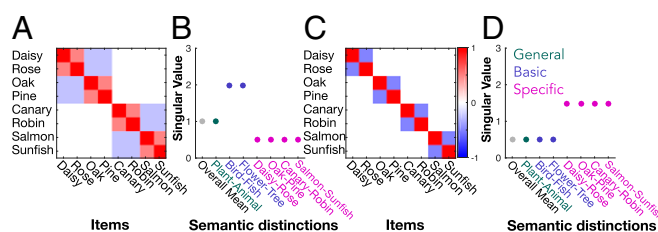


Fig. 8. From similarity structure to category coherence. (A) A hierarchical similarity structure over objects in which categories at the basic level are very different from each other due to a negative similarity. (B) For this structure, basic-level categorical distinctions acquire larger singular values, or category coherence, and therefore gain an advantage in both learning and task performance. (C) Now, subordinate categories are very different from each other through negative similarity. (D) Consequently, subordinate categories gain a coherence advantage. See *SI Appendix* for formulas relating similarity structure to category coherence.

to share features. For each of these forms, in the limit of a large number of features, we compute the item–item covariance matrices (Fig. 9, second row), object-analyzer vectors (Fig. 9, third row), and singular values of the input–output correlation matrix, and we use them in Eq. 6 to compute the development of the network’s internal representations through Eq. 8, as shown in Fig. 9, bottom. Overall, this approach yields several insights into how distinct structural forms, through their different statistics, drive learning in a deep network, as summarized below.

Clusters. Graphs that break items into distinct clusters give rise to block-diagonal constant matrices, yielding object-analyzer vectors that pick out cluster membership.

Trees. Tree graphs give rise to ultrametric covariance matrices, yielding object-analyzer vectors that are tree-structured wavelets that mirror the underlying hierarchy (42, 43).

Rings and grids. Ring-structured graphs give rise to circulant covariance matrices, yielding object-analyzer vectors that are Fourier modes ordered from lowest to highest frequency (44).

Orderings. Graphs that transitively order items yield highly structured, but nonstandard, covariance matrices whose object analyzers encode the ordering.

Cross-cutting structure. Real-world domains need not have a single underlying structural form. For instance, while some features of animals and plants generally follow a hierarchical structure, other features, like male and female, can link together hierarchically disparate items. Such cross-cutting structure can be orthogonal to the hierarchical structure, yielding object-analyzer vectors that span hierarchical distinctions.

These results reflect an analytic link between two popular, but different, methods of capturing structure: PGMs and deep networks. This analysis transcends the particulars of any one dataset and shows how different abstract structures can become embedded in the internal representations of a deep neural network. Strikingly, the same generic network can accommodate all of these structure types, without requiring the set of possible candidate structures a priori.

Deploying Knowledge: Inductive Projection

Over the course of development, the knowledge children acquire powerfully reshapes their inductions upon encountering novel items and properties (2, 3). For instance, upon learning a novel fact (e.g., “a canary is warm-blooded”) children extend this new knowledge to related items, as revealed by their answers to questions like “is a robin warm-blooded?” Studies have shown that children’s answers to such questions change over the course of development (2, 3, 17–19), generally becoming more specific. For example, young children may project the novel property of warm-blooded to distantly related items, while older children will only project it to more closely related items. How could such changing patterns arise in a neural network? Here, building upon previous network simulations (4, 28), we show analytically that deep networks exposed to hierarchically structured data naturally yield

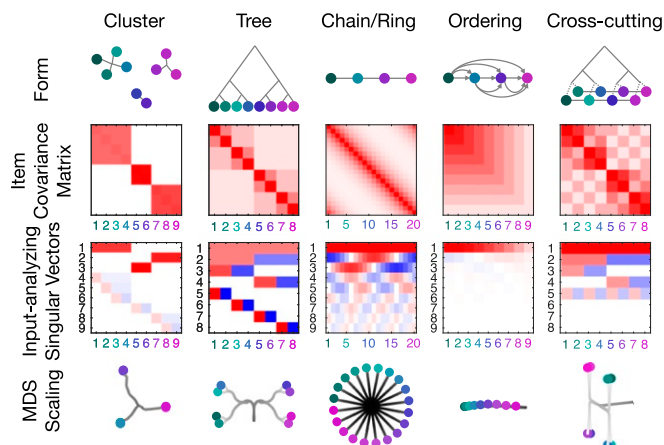


Fig. 9. Representation of explicit structural forms in a neural network. Each column shows a different structure. The first four columns correspond to pure structural forms, while the final column has cross-cutting structure. First row: The structure of the data generating PGM. Second row: The resulting item-covariance matrix arising from either data drawn from the PGM (first four columns) or designed by hand (final column). Third row: The input-analyzing singular vectors that will be learned by the linear neural network. Each vector is scaled by its singular value, showing its importance to representing the covariance matrix. Fourth row: MDS view of the development of internal representations.

progressively narrowing patterns of inductive projection across development.

Consider the act of learning that a familiar item has a novel feature (e.g., “a pine has property x ”). To accommodate this knowledge, new synaptic weights must be chosen between the familiar item *pine* and the novel property x (Fig. 10A), without disrupting prior knowledge of items and their properties already stored in the network. This may be accomplished by adjusting only the weights from the hidden layer to the novel feature so as to activate it appropriately. With these new weights established, inductive projections of the novel feature to other familiar items (e.g., “does a rose have property x ?”) naturally arise by querying the network with other inputs. If a novel property m is ascribed to a familiar item i , the inductive projection of this property to any other item j is given by (SI Appendix)

$$\hat{y}_m = \mathbf{h}_j^T \mathbf{h}_i / \|\mathbf{h}_i\|^2. \quad [16]$$

This equation implements a similarity-based inductive projection to other items, where the similarity metric is precisely the Euclidean similarity of hidden representations of pairs of items (Fig. 10B). In essence, being told “a pine has property x ,” the network will more readily project the novel property x to those familiar items whose hidden representations are close to that of the pine.

A parallel situation arises upon learning that a novel item possesses a familiar feature (e.g., “a blink can move”; Fig. 10C). Encoding this knowledge requires new synaptic weights between the item and the hidden layer. Appropriate weights may be found through standard gradient descent learning of the item-to-hidden weights for this novel item, while holding the hidden-to-output weights fixed to preserve prior knowledge about features. The network can then project other familiar properties to the novel item (e.g., “Does a blink have legs?”) by simply generating a feature output vector given the novel item as input. A novel item i with a familiar feature m will be assigned another familiar feature n through (SI Appendix)

$$\hat{y}_n = \mathbf{h}_n^T \mathbf{h}_m / \|\mathbf{h}_m\|^2, \quad [17]$$

where the α^{th} component of \mathbf{h}_n is $\mathbf{h}_n^\alpha = \mathbf{u}_n^\alpha \sqrt{a_\alpha(t)}$. $\mathbf{h}_n \in \mathbb{R}^{N_2}$ can be thought of as the hidden representation of feature n

at developmental time t . In parallel to [16], this equation now implements similarity-based inductive projection of familiar features to a novel item. In essence, by being told “a blink can move,” the network will more readily project other familiar features to a blink, if those features have a similar internal representation as that of the feature move.

Thus, the hidden layer of the deep network furnishes a common, semantic representational space into which both features and items can be placed. When a novel feature m is assigned to a familiar item i , that novel feature is placed close to the familiar item in the hidden layer, and so the network will inductively project this novel feature to other items close to i in neural space. In parallel, when a novel item i is assigned a familiar feature m , that novel item is placed close to the familiar feature, and so the network will inductively project other features close to m in neural space onto the novel item.

This principle of similarity-based generalization encapsulated in Eqs. 16 and 17, when combined with the progressive differentiation of internal representations as the network learns from hierarchically structured data, as illustrated in Fig. 2B, then naturally explains the developmental shift in patterns of inductive projection from broad to specific, as shown in Fig. 10E. For example, consider specifically the inductive projection of a novel feature to familiar items (Fig. 10A and B). Earlier (later) in developmental time, neural representations of all items are more similar to (different from) each other, and so the network’s similarity-based inductive projection will extend the novel feature to many (fewer) items, thereby exhibiting progressively narrower patterns of projection that respect the hierarchical structure of the environment (Fig. 10E). Thus, remarkably, even a deep linear network can provably exhibit the same broad to specific changes in patterns of inductive projection, empirically observed in many works (2, 3, 17, 18).

Linking Behavior and Neural Representations

Compared with previous models which have primarily made behavioral predictions, our theory has a clear neural

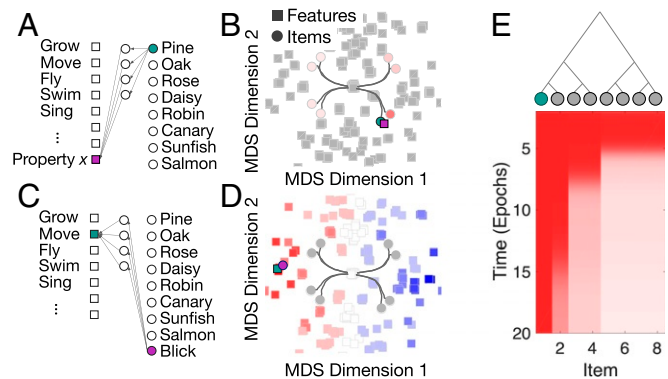


Fig. 10. The neural geometry of inductive generalization. (A) A novel feature (property x) is observed for a familiar item (e.g., “a pine has property x ”). (B) Learning assigns the novel feature a neural representation in the hidden layer of the network that places it in semantic similarity space near the object which possesses the novel feature. The network then inductively projects that novel feature to other familiar items (e.g., “Does a rose have property x ?”) only if their hidden representation is close in neural space. (C) A novel item (a blink) possesses a familiar feature (e.g., “a blink can move”). (D) Learning assigns the novel item a neural representation in the hidden layer that places it in semantic similarity space near the feature possessed by the novel item. Other features are inductively projected to that item (e.g., “Does a blink have wings?”) only if their hidden representation is close in neural space. (E) Inductive projection of a novel property (“a pine has property x ”) over learning. As learning progresses, the neural representations of items become progressively differentiated, yielding progressively restricted projection of the novel feature to other items. Here, the pine can be thought of as the left-most item node in the tree.

interpretation. Here, we discuss implications for the neural basis of semantic cognition.

Similarity Structure Is an Invariant of Optimal Learning. An influential method for probing neural codes for semantic knowledge in empirical measurements of neural activity is the representational similarity approach (20, 21, 25, 45), which examines the similarity structure of neural population vectors in response to different stimuli. This technique has identified rich structure in high-level visual cortices, where, for instance, inanimate objects are differentiated from animate objects (22, 23). Strikingly, studies have found remarkable constancy between neural similarity structures across human subjects and even between humans and monkeys (24, 25). This highly conserved similarity structure emerges, despite considerable variability in neural activity patterns across subjects (46, 47). Indeed, exploiting similarity structure enables more effective across-subject decoding of fMRI data relative to transferring a decoder based on careful anatomical alignment (48). Why is representational similarity conserved, both across individuals and species, despite highly variable tuning of individual neurons and anatomical differences?

Remarkably, we show that two networks trained in the same environment must have identical representational similarity matrices, despite having detailed differences in neural tuning patterns, provided that the learning process is optimal, in the sense that it yields the smallest norm weights that solve the task (see *SI Appendix*). One way to get close to the optimal manifold of smallest norm synaptic weights after learning is to start learning from small random initial weights. We show in Fig. 11 *A* and *B* that two networks, each starting from different sets of small random initial weights, will learn very different internal representations (Fig. 11 *A* and *B*, *Top*), but will have nearly identical representational similarity matrices (Fig. 11 *A* and *B*, *Middle*). Such a result is, however, not obligatory. Two networks starting from large random initial weights not only learn different internal representations, but also learn different representational similarity matrices (Fig. 11 *C* and *D*, *Top* and *Middle*). This pair of networks both learns the same composite input-output map, but with suboptimal large-norm weights. Hence, our theory, combined with the empirical finding that similarity structure is preserved across humans and species, suggests these disparate neural circuits may be implementing approximately optimal learning in a common environment.

When the Brain Mirrors Behavior. In addition to matching neural similarity patterns across subjects, experiments using fMRI and single-unit responses have also documented a correspondence between neural similarity patterns and behavioral similarity patterns (21). When does neural similarity mirror behavioral similarity? We show this correspondence again emerges only in optimal networks. In particular, denote by $\hat{\mathbf{y}}_i$ the behavioral output of the network in response to item i . These output patterns yield the behavioral similarity matrix $\Sigma^{\hat{\mathbf{y}}} = \hat{\mathbf{y}}_i^T \hat{\mathbf{y}}_j$. In contrast, the neural similarity matrix is $\Sigma^{\mathbf{h}} = \mathbf{h}_i^T \mathbf{h}_j$, where \mathbf{h}_i is the hidden representation of stimulus i . We show in *SI Appendix* that if the network learns optimal smallest norm weights, then these two similarity matrices obey the relation $\Sigma^{\hat{\mathbf{y}}} = (\Sigma^{\mathbf{h}})^2$, and therefore share the same singular vectors. Hence, behavioral-similarity patterns share the same structure as neural-similarity patterns, but with each semantic distinction expressed more strongly (according to the square of its singular value) in behavior relative to the neural representation. While this precise mathematical relation is yet to be tested in detail, some evidence points to this greater category separation in behavior (24).

Given that optimal learning is a prerequisite for neural similarity mirroring behavioral similarity, as in the previous section, there is a match between the two for pairs of networks trained from small random initial weights (Fig. 11 *A* and *B*, *Middle* and *Bottom*), but not for pairs of networks trained from large random

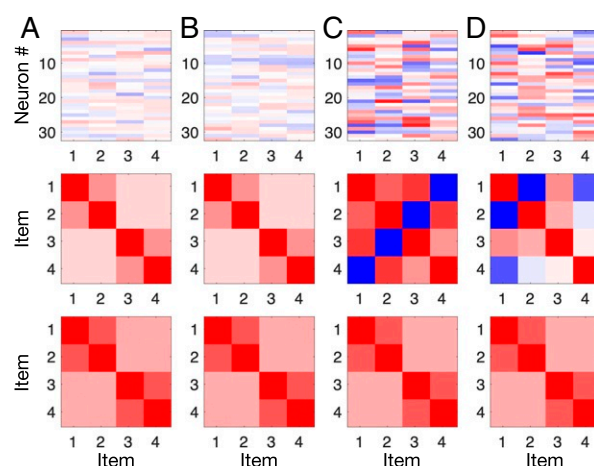


Fig. 11. Neural representations and invariants of learning. *A* and *B* depict two networks trained from small norm random weights. *C* and *D* depict two networks trained from large norm random weights. (*Top*) Neural tuning curves \mathbf{h}_i at the end of learning. Neurons show mixed selectivity tuning, and individual tuning curves are different for different trained networks. (*Middle*) Representational similarity matrix $\Sigma^{\mathbf{h}}$. (*Bottom*) Behavioral similarity matrix $\Sigma^{\mathbf{y}}$. For small-norm, but not large-norm, weight initializations, representational similarity is conserved, and behavioral similarity mirrors neural similarity.

initial weights (Fig. 11 *C* and *D*, *Middle* and *Bottom*). Thus, again, speculatively, our theory suggests that the experimental observation of a link between behavioral and neural similarity may in fact indicate that learning in the brain is finding optimal network solutions that efficiently implement the requisite transformations with minimal synaptic strengths.

Discussion

In summary, the main contribution of our work is the analysis of a simple model—namely, a deep linear neural network—that can, surprisingly, qualitatively capture a diverse array of phenomena in semantic development and cognition. Our exact analytical solutions of nonlinear learning phenomena in this model yield conceptual insights into why such phenomena also occur in more complex nonlinear networks (4, 28–32) trained to solve semantic tasks. In particular, we find that the hierarchical differentiation of internal representations in a deep, but not a shallow, network (Fig. 2) is an inevitable consequence of the fact that singular values of the input-output correlation matrix drive the timing of rapid developmental transitions (Fig. 3 and Eqs. 6 and 10), and hierarchically structured data contain a hierarchy of singular values (Fig. 4). In turn, semantic illusions can be highly prevalent between these rapid transitions simply because global optimality in predicting all features of all items necessitates sacrificing correctness in predicting some features of some items (Fig. 5). And, finally, this hierarchical differentiation of concepts is intimately tied to the progressive sharpening of inductive generalizations made by the network (Fig. 10).

The encoding of knowledge in the neural network after learning also reveals precise mathematical definitions of several aspects of semantic cognition. Basically, the synaptic weights of the neural network extract from the statistical structure of the environment a set of paired object analyzers and feature synthesizers associated with every categorical distinction. The bootstrapped, simultaneous learning of each pair solves the apparent Gordian knot of knowing both which items belong to a category and which features are important for that category: The object analyzers determine category membership, while the feature synthesizers determine feature importance, and the set of extracted categories are uniquely determined by the statistics of the environment. Moreover, by defining the typicality of an item for a category as the strength of that item in the

category's object analyzer, we can prove that typical items must enjoy enhanced performance in semantic tasks relative to atypical items (Eq. 12). Also, by defining the category prototype to be the associated feature synthesizer, we can prove that the most typical items for a category are those that have the most extremal projections onto the category prototype (Fig. 6 and Eq. 13). Finally, by defining the coherence of a category to be the associated singular value, we can prove that more coherent categories can be learned more easily and rapidly (Fig. 7) and explain how changes in the statistical structure of the environment determine what level of a category hierarchy is the most basic or important (Fig. 8). All our definitions of typicality, prototypes, and category coherence are broadly consistent with intuitions articulated in a wealth of psychology literature, but our definitions imbue these intuitions with enough mathematical precision to prove theorems connecting them to aspects of category learnability, learning speed, and semantic task performance in a neural network model.

More generally, beyond categorical structure, our analysis provides a principled framework for explaining how the statistical structure of diverse structural forms associated with different PGMs gradually becomes encoded in the weights of a neural network (Fig. 9). Remarkably, the network learns these structures without knowledge of the set of candidate structural forms, demonstrating that such forms need not be built in. Regarding neural representation, our theory reveals that, across different networks trained to solve a task, while there may be no correspondence at the level of single neurons, the similarity structure

of internal representations of any two networks will both be identical to each other and closely related to the similarity structure of behavior, provided that both networks solve the task optimally, with the smallest possible synaptic weights (Fig. 11).

While our simple neural network captures this diversity of semantic phenomena in a mathematically tractable manner, because of its linearity, the phenomena it can capture still barely scratch the surface of semantic cognition. Some fundamental semantic phenomena that require complex nonlinear processing include context-dependent computations, dementia in damaged networks, theory of mind, the deduction of causal structure, and the binding of items to roles in events and situations. While it is inevitably the case that biological neural circuits exhibit all of these phenomena, it is not clear how our current generation of artificial nonlinear neural networks can recapitulate all of them. However, we hope that a deeper mathematical understanding of even the simple network presented here can serve as a springboard for the theoretical analysis of more complex neural circuits, which, in turn, may eventually shed much-needed light on how the higher-level computations of the mind can emerge from the biological wetware of the brain.

ACKNOWLEDGMENTS. We thank Juan Gao and Madhu Advani for useful discussions. S.G. was supported by the Burroughs-Wellcome, Sloan, McKnight, James S. McDonnell, and Simons foundations. J.L.M. was supported by the Air Force Office of Scientific Research. A.M.S. was supported by Swartz, National Defense Science and Engineering Graduate, and Mind, Brain, & Computation fellowships.

- Keil F (1979) *Semantic and Conceptual Development: An Ontological Perspective* (Harvard Univ Press, Cambridge, MA).
- Carey S (1985) *Conceptual Change In Childhood* (MIT Press, Cambridge, MA).
- Murphy G (2002) *The Big Book of Concepts* (MIT, Cambridge, MA).
- Rogers TT, McClelland JL (2004) *Semantic Cognition: A Parallel Distributed Processing Approach* (MIT Press, Cambridge, MA).
- Mandler J, McDonough L (1993) Concept formation in infancy. *Cogn Dev* 8:291–318.
- Inhelder B, Piaget J (1958) *The Growth of Logical Thinking from Childhood to Adolescence* (Basic Books, New York).
- Siegler R (1976) Three aspects of cognitive development. *Cogn Psychol* 8:481–520.
- Rosch E, Mervis C (1975) Family resemblances: Studies in the internal structure of categories. *Cogn Psychol* 7:573–605.
- Barsalou L (1985) Ideals, central tendency, and frequency of instantiation as determinants of graded structure in categories. *J Exp Psychol Learn Mem Cogn* 11: 629–654.
- Rips L, Shoben E, Smith E (1973) Semantic distance and the verification of semantic relations. *J Verbal Learn Verbal Behav* 12:1–20.
- Murphy G, Brownell H (1985) Category differentiation in object recognition: Typicality constraints on the basic category advantage. *J Exp Psychol Learn Mem Cogn* 11:70–84.
- Mervis C, Catlin J, Rosch E (1976) Relationships among goodness-of-example, category norms, and word frequency. *Bull Psychon Soc* 7:283–284.
- Rips L (1975) Inductive judgments about natural categories. *J Verbal Learn Verbal Behav* 14:665–681.
- Osherson D, Smith E, Wilkie O, López A, Shafir E (1990) Category-based induction. *Psychol Rev* 97:185–200.
- Rosch E (1978) *Principles of Categorization in Cognition and Categorization*, eds Rosch E, Lloyd B (Lawrence Erlbaum, Hillsdale, NJ), pp 27–48.
- Murphy G, Medin D (1985) The role of theories in conceptual coherence. *Psychol Rev* 92:289–316.
- Keil F (1991) The emergence of theoretical beliefs as constraints on concepts. *The Epigenesis of Mind: Essays on Biology and Cognition*, eds Carey S, Gelman R (Psychology Press, New York).
- Carey S (2011) Précis of 'the origin of concepts'. *Behav Brain Sci* 34:113–124.
- Gelman S, Coley J (1990) The importance of knowing a dodo is a bird: Categories and inferences in 2-year-old children. *Dev Psychol* 26:796–804.
- Edelman S (1998) Representation is representation of similarities. *Behav Brain Sci* 21:449–467.
- Kriegeskorte N, Kievit R (2013) Representational geometry: Integrating cognition, computation, and the brain. *Trends Cogn Sci* 17:401–412.
- Carlson T, Simmons R, Kriegeskorte N, Slevc L (2014) The emergence of semantic meaning in the ventral temporal pathway. *J Cogn Neurosci* 26:120–131.
- Connolly A, et al. (2012) The representation of biological classes in the human brain. *J Neurosci* 32:2608–2618.
- Mur M, et al. (2013) Human object-similarity judgments reflect and transcend the primate-IT object representation. *Front Psychol* 4:128.
- Kriegeskorte N, et al. (2008) Matching categorical object representations in inferior temporal cortex of man and monkey. *Neuron* 60:1126–1141.
- Kemp C, Tenenbaum J (2008) The discovery of structural form. *Proc Natl Acad Sci USA* 105:10687–10692.
- Hinton G (1986) Learning distributed representations of concepts. *Parallel Distributed Processing: Implications for Psychology and Neurobiology*, ed Morris R (Oxford Univ Press, Oxford).
- Rumelhart D, Todd P (1993) *Learning and Connectionist Representations in Attention and Performance XIV*, eds Meyer D, Kornblum S (MIT Press, Cambridge, MA).
- McClelland J (1995) A connectionist perspective on knowledge and development. *Developing Cognitive Competence: New Approaches to Process Modeling*, eds Simon T, Halford G (Erlbaum, Hillsdale, NJ).
- Plunkett K, Sinha C (1992) Connectionism and developmental theory. *Br J Dev Psychol* 10:209–254.
- Quinn P, Johnson M (1997) The emergence of perceptual category representations in young infants. *J Exp Child Psychol* 66:236–263.
- Colunga E, Smith L (2005) From the lexicon to expectations about kinds: A role for associative learning. *Psychol Rev* 112:347–382.
- Poole B, Lahiri S, Raghu M, Sohl-Dickstein J, Ganguli S (2016) Exponential expressivity in deep neural networks through transient chaos. *Advances in Neural Information Processing Systems*, eds Lee D, Sugiyama M, Luxburg U, Guyon I, Garnett R (MIT Press, Cambridge, MA), Vol 29, pp 3360–3368.
- Gelman R (1990) First principles organize attention to and learning about relevant data: Number and the animate-inanimate distinction as examples. *Cogn Sci* 14:79–106.
- Mervis C, Crisafi M (1982) Order of acquisition of subordinate-, basic-, and superordinate-level categories. *Child Dev* 53:258–266.
- Davis T, Poldrack R (2014) Quantifying the internal structure of categories using a neural typicality measure. *Cereb Cortex* 24:1720–1737.
- Rosch E, Simpson C, Miller R (1976) Structural bases of typicality effects. *J Exp Psychol Hum Percept Perform* 2:491–502.
- Anglin J (1977) *Word, Object, and Conceptual Development* (Norton, New York), p 302.
- Rosch E, Mervis C, Gray W, Johnson D, Boyes-Braem P (1976) Basic objects in natural categories. *Cogn Psychol* 8:382–439.
- Mandler J, Bauer P, McDonough L (1991) Separating the sheep from the goats: Differentiating global categories. *Cogn Psychol* 23:263–298.
- Cortez J, Gluck M (1992) Explaining basic categories: Feature predictability and information. *Psychol Bull* 111:291–303.
- Khrennikov A, Kozyrev S (2005) Wavelets on ultrametric spaces. *Appl Comput Harmon Anal* 19:61–76.
- Murtagh F (2007) The Haar wavelet transform of a dendrogram. *J Classif* 24:3–32.
- Gray R (2005) Toeplitz and circulant matrices: A review. *Foundations Trends Communications Information Theory* 2:155–239.
- Laakso A, Cottrell G (2000) Content and cluster analysis: Assessing representational similarity in neural systems. *Philos Psychol* 13:47–76.
- Haxby J, et al. (2001) Distributed and overlapping representations of faces and objects in ventral temporal cortex. *Science* 293:2425–2430.
- Shinkareva S, Malave V, Just M, Mitchell T (2012) Exploring commonalities across participants in the neural representation of objects. *Hum Brain Mapp* 33:1375–1383.
- Raizada R, Connolly A (2012) What makes different people's representations alike: Neural similarity space solves the problem of across-subject fMRI decoding. *J Cogn Neurosci* 24:868–877.